Steel and Composite Structures, *Vol. 33, No. 1* (*2019*) *67-79*
DOI: https://doi.org/10.12989/scs.2019.33.1.067

Experimental and analytical investigation of composite columns made of high strength steel and high strength concrete

Binglin Lai [1], J.Y. Richard Liew*[1,2] and Mingxiang Xiong [3,1]

[1] *Department of Civil and Environmental Engineering, National University of Singapore, Blk E1A, #07-03, 1 Engineering Drive 2, 117576, Singapore*
[2] *School of Civil Engineering, NanjingTech University, No. 30 Puzhu Road(S), Nanjing 211816, China*
[3] *Protective Structures Centre, School of Civil Engineering, Guangzhou University, Guangzhou, China*

(*Received January 24, 2019, Revised August 20, 2019, Accepted September 25, 2019*)

Abstract. Composite columns made of high strength materials have been used in high-rise construction owing to its excellent structural performance resulting in smaller cross-sectional sizes. However, due to the limited understanding of its structural response, current design codes do not allow the use of high strength materials beyond a certain strength limit. This paper reports additional test data, analytical and numerical studies leading to a new design method to predict the ultimate resistance of composite columns made of high strength steel and high strength concrete. Based on previous study on high strength concrete filled steel tubular members and ongoing work on high strength concrete encased steel columns, this paper provides new findings and presents the feasibility of using high strength steel and high strength concrete for general double symmetric composite columns. A nonlinear finite element model has been developed to capture the composite beam-column behavior. The Eurocode 4 approach of designing composite columns is examined by comparing the test data with results obtained from code's predictions and finite element analysis, from which the validities of the concrete confinement effect and plastic design method are discussed. Eurocode 4 method is found to overestimate the resistance of concrete encased composite columns when ultra-high strength steel is used. Finally, a strain compatibility method is proposed as a modification of existing Eurocode 4 method to give reasonable prediction of the ultimate strength of concrete encased beam-columns with steel strength up to 900 MPa and concrete strength up to 100 MPa.

Keywords: concrete filled columns; concrete encased column; Eurocode 4; high strength steel; high strength concrete; strain compatibility method; tall buildings

1. Introduction

Composite column is a type of structural form which maximizes the benefits of steel and concrete materials to achieve desired structural performance and efficiency. As compared with conventional steel columns and Reinforced Concrete (RC) columns, composite column offers advantages in terms of high stiffness and high strength, hence the member size can be reduced accordingly and permit the utilization of more open space. Based on different structural configuration, the most typical forms of composite column can be categorized as Concrete Filled Steel Tubular (CFST) columns and Concrete Encased Steel (CES) columns as sketched in Fig. 1. CFST columns greatly save construction time since the outer tube serves as permanent formwork for the infilled concrete, and the confining pressure provided by steel tube does improve strength and ductility. In order to guarantee fire resistance, concrete core can be reinforced with steel fibres and inner steel section as an alternative to longitudinal reinforce-ments. CES column is another form having the same overall configuration as RC column except for the placement of steel section inside. Different from CFST columns, the surrounding concrete encasement protects the steel core against fire and local buckling; hence thinner steel plate is allowed to be used regardless of the section's plate slenderness ratio.

However, modern design codes do not cover the design of composite columns using high strength materials (EN1994-1-1 2004, JGJ 138-2016 2016, ANSI/AISC 360-16 2016, AIJ 1997). As tabulated in Table. 1, most existing design provisions impose certain limitation on material strength due to insufficient experimental research at that time. In the past years, experimental and numerical studies have been conducted (Xiong *et al*. 2017a, b, Du *et al*. 2016, 2017, Han *et al*. 2001, 2007, Lam and Williams 2004, Uy 2001, Johansson and Gylltoft 2001, Chen and Yeh 1996, Tsai *et al*. 1996, Chen and Lin 2006, Fenollosa *et al*. 2015, Roik and Bergmann 1990, Lai *et al*. 2018, Hanswille *et al*. 2017, Tokgoz and Dundar 2008) to investigate structural performance of normal strength and high strength composite columns, and a database has been established based on test data from thepublished literatures (Xiong *et al*. 2017b, Liew *et al*. 2016, Kim 2005). From research to practice, Liew and Xiong (2015) developed a new design guide applicable to CFST members with concrete grade up to C90/105 and steel grade up to S550, and proposed the matching grade of steel and concrete with the purpose of ensuring full plastic resistance.

*Corresponding author, Professor,
E-mail: ceeljy@nus.edu.sg

ISSN: 1229-9367 (Print), 1598-6233 (Online)

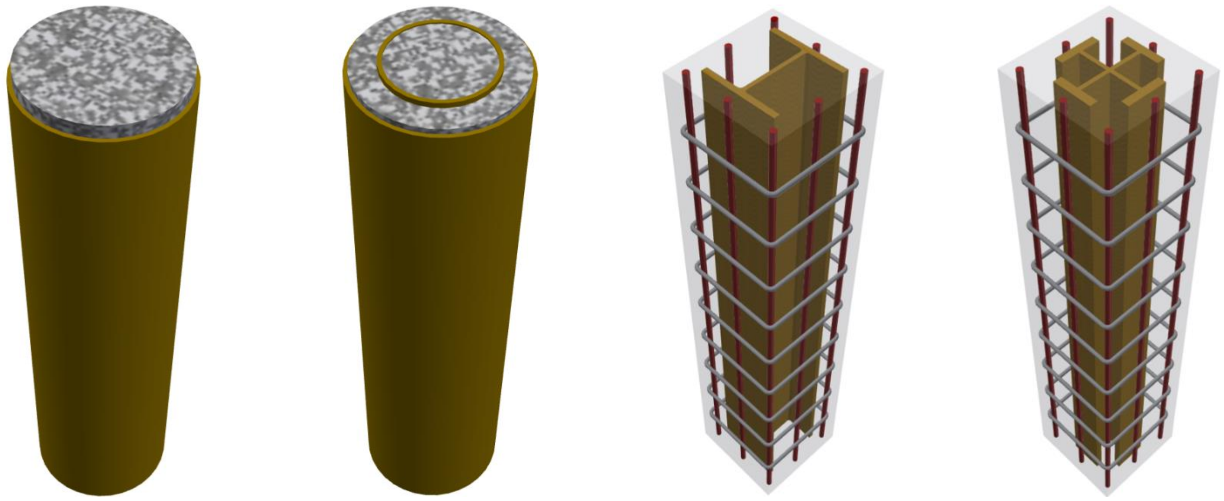

Fig. 1 General types of composite columns

As shown in Figs. 2 and 3, comparing with CFST columns, experimental study on CES columns is quite limited and most of them focused on normal strength materials (Chen and Yeh 1996, Tsai *et al*. 1996, Chen and Lin 2006, Tokgoz and Dundar 2008, Munoz and Hsu 1997), only 9.3% of tests were carried out on columns with concrete compressive strength greater than 50 MPa, and high strength (> 460 MPa) just account for 5.4% of all test data. Chen and Yeh (1996) and Tsai *et al*. (1996) carried out a series of physical tests on normal strength CES columns reinforced with H-shaped and cruciform steel section, based on which Chen and Lin (2006) developed an analytical model capable of predicting the axial capacity of CES stub columns by dividing the concrete zone into three different regions according to different confinement degree. Some new design methods (Fenollosa *et al*. 2015, Roik and Bergmann 1990, Lai *et al*. 2018, Hanswille *et al*. 2017) have been developed to deal with special composite columns not covered in existing EC4, including CES columns with non-symmetric cross-section and CFST columns with massive inner cores. Tokgoz and Dundar (2008) and Munoz and Hsu (1997) conducted research on biaxially loaded CES beam-columns and proposed simplified equations to construct M-N interaction diagrams under biaxial bending. Numerical studies on CES columns were undertaken by El-Tawil and Deierlein (1999) and Ellobody *et al*. (2011), in which fibre element method and finite element method were employed, respectively. For high strength CES columns, to the best knowledge of the authors, test results reported in Zhu *et al*. (2014) and Kim *et al*. (2011, 2013) were the only test data available from published literature. Zhu *et al*. (2014) investigated the axial capacity of CES stub columns with high strength concrete C90 and normal strength steel S235 while Kim *et al*. (2011, 2013) conduct eccentric test on CES beam-column with high strength concrete C100 and ultrahigh strength steel S900. Despite these available researches on high strength CES column, the structural behaviors including deformation response, failure mechanism, confinement requirement, and the synergistic effect between high strength steel high strength concrete etc., still remains not fully understood. Therefore, more experimental and numerical work are needed to facilitate the design guide of high strength CES columns.

Table 1 Limitations on material strength for composite columns design

Codes	Concrete strength	Steel strength
	(N/mm^2)	(N/mm^2)
EN 1992-1-1: 2004	N.A.	12-90
EN 1993-1-1: 2005	235-700	N.A.
EN 1994-1-1: 2005	235-460	25-50[a]
AIJ (1997)	235-440	18-90[a]
JGJ 138-2016	235-420	20-80[b]
AISC 360-16: 2016	$\leq$ 525	21-69[a]

[a] denotes concrete cylinder strength;
[b] denotes concrete cubic strength

To continue the previous research (Xiong *et al*. 2017a, b) on CFST columns, this paper presents new findings on high strength CES members through experimental, analytical and numerical investigation. Existing Eurocode 4 (2004) method is carefully examined in predicting axial cross-section resistance, buckling resistance and beam-column resistance. Finally, a new method is proposed to construct the cross-sectional M-N interaction diagrams in a proper way complying with material compatibility requirement proposed by Liew *et al*. (Liew and Xiong 2015, Liew *et al*. 2016). A direct second order analysis may be carried to analyze the composite beam-columns with initial imperfections to determine the maximum design moment (Liu *et al*. 2012). Cross section capacity check is then carried out to ensure the design forces are within the axial-moment interaction curve developed from the proposed method.

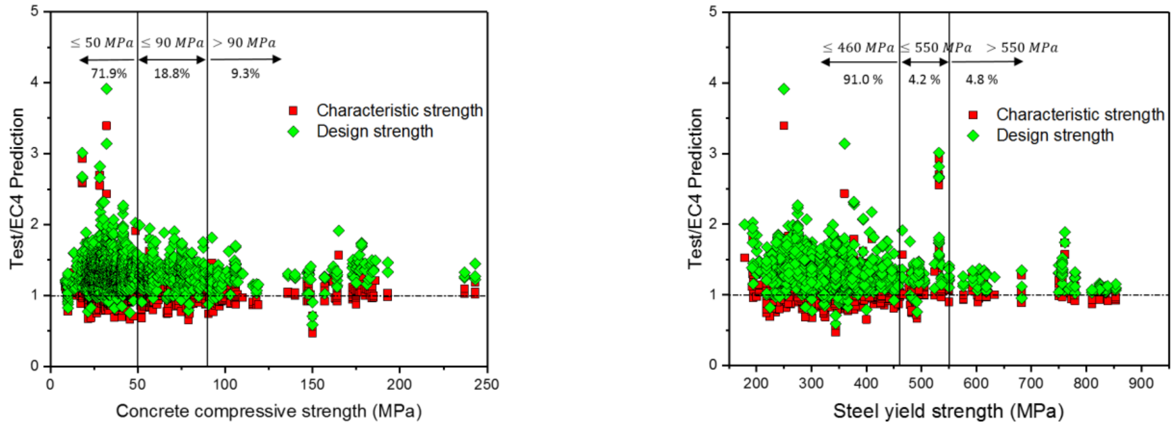

Fig. 2 Comparison of test/EC4 prediction ratio against material strength for CFST columns (Liew *et al*. 2016)

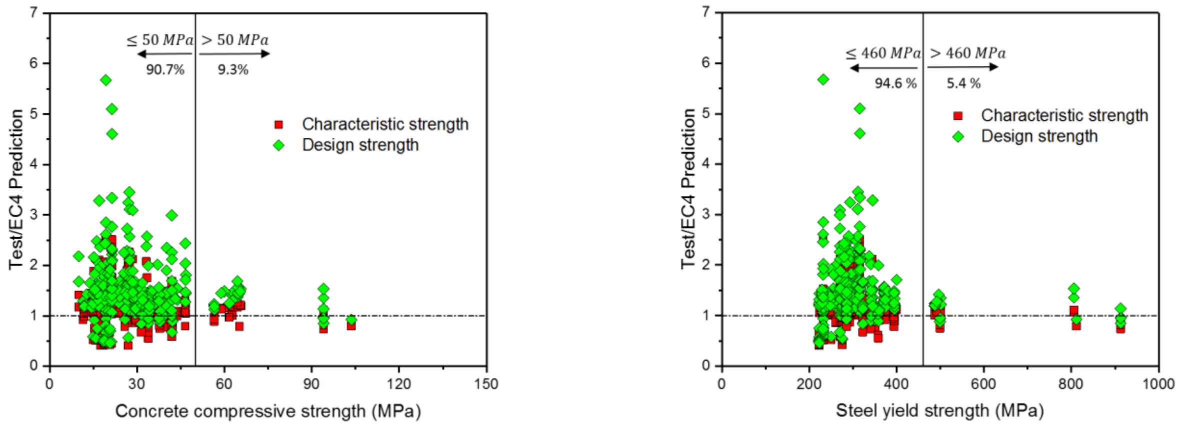

Fig. 3 Comparison of test/EC4 prediction ratio against material strength for CES columns

2. Prediction based on Eurocode's method

Eurocode 4 (EC4) permits the design of composite columns with concrete grade from C20/25 to C50/60 and steel grade from S235 to S460, of which the feasibility has been validated through numerous experimental and numerical study (Han *et al*. 2001, 2007, Lam and Williams 2004, Johansson and Gylltoft 2001, Chen and Yeh 1996, Tsai *et al*. 1996, Chen and Lin 2006, Fenollosa *et al*. 2015, Roik and Bergmann 1990). For the design of CES columns, EC4 simplified method is only applicable when steel contribution ratio ranges from 0.2 to 0.9, beyond which it shall be treated as bare steel columns or Reinforced Concrete (RC) columns, hence Eurocode 2 or Eurocode 3 shall be employed. In order to prevent local buckling in CES column, cover thickness of steel profile shall be greater than 40 mm, while it must be less than 30% of steel section height along the minor axis and 40% of web width along the major axis to ensure the development of plastic strength. Since slender members may suffer from instability failure, composite columns with non-dimensional slenderness ratio exceeding 2.0 were beyond scope of EC4 simplified method.

Generally speaking, EC4 simplified method is more commonly adopted in practical design than the general method, however the former is limited to members with double symmetrical and constant cross-section along member length, otherwise general method shall be used, but EC4 does not provide explicit provisions in dealing with those irregular columns. Lai *et al*. (2018) proposed a method applicable to predict cross-section capacity of CES columns with off-center steel section.

2.1 Cross-section resistance under pure compression

Based on the condition that steel yielding occurs before concrete reaches the maximum stress, Eurocode 4 adopts plastic design philosophy in the examination of bearing capacity, and the composite actions between constituent materials were implicitly considered by assuming perfect bond in the steel-concrete interface and the incorporation of concrete confinement effect in CFST columns. In the estimation of cross-section resistance under pure compression, superposition principle is used in EC4 and formulated as below

CES column $$N_{pl,Rd} = A_a f_{yd} + 0.85 A_c f_{cd} + A_s f_{sd} \quad (1)$$

Square CFST column $$N_{pl,Rd} = A_a f_{yd} + 1.0 A_c f_{cd} + A_s f_{sd} \quad (2)$$

where $N_{pl,Rd}$ refers to plastic resistance of composite cross-section under pure compression. A_a, A_c and A_s refers to cross-section area of steel section, concrete and longitudinal reinforcement, f_{yd}, f_{cd} and f_{sd} refers to the design strength of steel section, concrete and longitudinal reinforcement bars, respectively. For CFST columns with circular cross-sections, confinement effect shall be reasonably taken into account provided that relative slenderness ratio and load eccentricity satisfy the requirement stated in EN 1994-1-1 (2004).

2.2 Bucking resistance under axial compression

Composite long columns under pure compression can be assessed using the second-order analysis by taking into account of member equivalent imperfection. For simplification, Buckling Curve Method (BCM) is often adopted by incorporating imperfection factor α to account for all possible geometric and structural imperfections, which is associate with cross-section type and flexure plane. The equations for computing buckling resistanceare given as follow

$$\bar{\lambda} = \sqrt{N_{pl,Rk}/N_{cr}} \tag{3}$$

$$\varphi = 0.5[1 + \alpha(\bar{\lambda} - 0.2) + \bar{\lambda}^2] \tag{4}$$

$$\chi = \frac{1}{\varphi + \sqrt{\varphi^2 - \bar{\lambda}^2}} \tag{5}$$

$$N_{bl,EC4} = \chi N_{Pl,Rd} \tag{6}$$

where $N_{pl,Rk}$ is squash load of CES columns, $N_{pl,Rk}$ = $0.85A_cf_c+A_{ss}f_{ys}+A_{sl}f_{yl}$. N_{cr} is Euler elastic buckling load computed as $N_{cr} = \pi^2EI_{eff}/(KL)^2$. $EI_{eff} = 0.6E_{cm}I_c + E_{ss}I_{ss} + E_{sl}I_{sl}$. K is buckling length factor taken as 1.0 for hinged columns.

2.3 Cross-section resistance under combining axial force and bending moment

The cross-sectional resistance of composite columns subjected to combining axial compression and bending moment can be approximated as polygonal diagrams as depicted in Fig. 4, which is constructed by connecting several anchor points with straight lines. In Eurocode 4, plastic stress distribution is assumed over the whole section, hence the yield strength of both structural steel and reinforcement are used for calculation, while the concrete strength remains as $0.85f_c$. For a given neutral axis location, axial force and bending moment resistance can be computed by integrating the stress block, and the bending moment-axial force (M-N) interaction diagrams can be generated by shifting the neutral axis consecutively. If the externally applied axis load and bending moment are within the envelope of interaction diagram, the column is able to resist the design forces, otherwise column will fail.

3. Test data on high strength Concrete Filled Steel Tubular (CFST) columns

Structural behavior of CFST columns with high strength and ultrahigh strength materials has been experimentally studied (Xiong *et al*. 2017a, b). A total of more than 40 specimens including stub columns and slender columns have been tested under concentric and eccentric compression. Specimen details are tabulated in Table 2 with double-tube and steel hollow sections excluded.

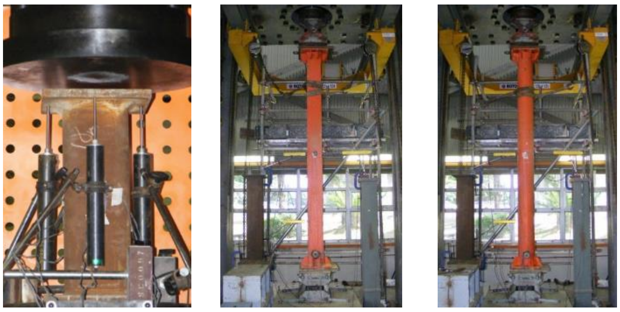

Short column Square beam-column Circular beam-column

Fig. 5 Test set-up and instrumentation for short columns and long columns (Xiong *et al*. 2017a, b)

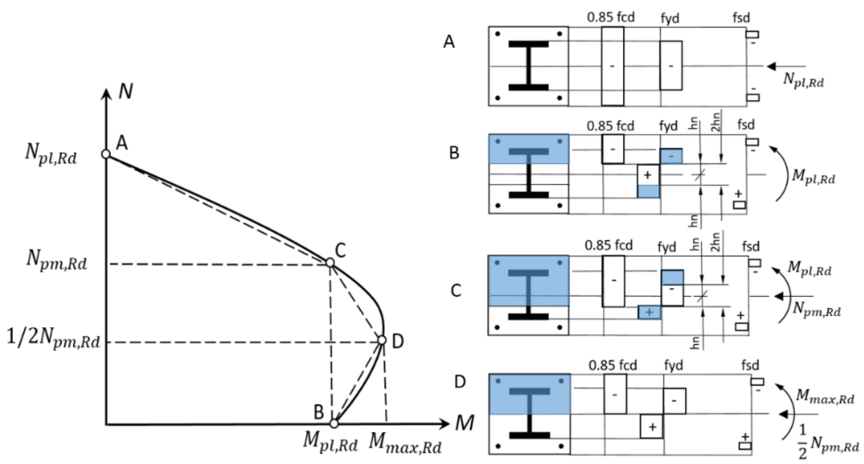

Fig. 4 Simplified axial force-bending moment interaction diagram and corresponding stress distribution

Table 2 Details of high strength CFST columns specimens (Xiong *et al*. 2017a, b)

Ref.	Specimen	Steel tube	f_{ys} (MPa)	E_s (GPa)	f_c (MPa)	E_c (GPa)	e_0 (mm)	L (mm)	λ
Xiong *et al*. 2017a	C3	CHS114.3 × 3.6	403	213	173.5	63	0	250	0.142
	C4	CHS114.3 × 3.6	403	213	173.5	63	0	250	0.142
	C5	CHS114.3 × 3.6	403	213	184.2	63	0	250	0.145
	C6	CHS114.3 × 3.6	403	213	184.2	63	0	250	0.145
	C7	CHS114.3 × 6.3	428	209	173.5	63	0	250	0.131
	C8	CHS114.3 × 6.3	428	209	173.5	63	0	250	0.131
	C10	CHS219.1 × 5	380	205	185.1	66	0	600	0.191
	C11	CHS219.1 × 5	380	205	193.3	67	0	600	0.193
	C13	CHS219.1 × 10	381	212	185.1	66	0	600	0.168
	C14	CHS219.1 × 10	381	212	193.3	67	0	600	0.170
	C15	CHS219.1 × 6.3	300	202	163	62	0	600	0.174
	C16	CHS219.1 × 6.3	300	202	175.4	58	0	600	0.181
	C17	CHS219.1 × 6.3	300	202	148.8	54	0	600	0.172
	C18	CHS219.1 × 6.3	300	202	174.5	56	0	600	0.182
	S1	SHS150 × 8	779	200	152.3	62	0	450	0.173
	S2	SHS150 × 8	779	200	157.2	58	0	450	0.175
	S3	SHS150 × 8	779	200	147	54	0	450	0.174
	S4	SHS150 × 8	779	200	164.1	58	0	450	0.177
	S5	SHS150 × 8	779	200	148	56	0	450	0.174
	S6	SHS150 × 12	756	200	152.3	62	0	450	0.171
	S7	SHS150 × 12	756	200	157.2	58	0	450	0.173
	S8	SHS150 × 12	756	200	147	54	0	450	0.172
	S9	SHS150 × 12	756	200	164.1	58	0	450	0.174
	S10	SHS150 × 12	756	200	148	56	0	450	0.172
	S11	SHS150 × 12.5	446	201	152.3	62	0	450	0.149
	S12	SHS150 × 12.5	446	201	157.2	58	0	450	0.151
	S13	SHS150 × 12.5	446	201	147	54	0	450	0.150
	S14	SHS150 × 12.5	446	201	164.1	58	0	450	0.153
	S15	SHS150 × 12.5	446	201	148	56	0	450	0.150
Xiong *et al*. 2017b	CS-1	CHS219.6 × 16	374	202	186	64.1	0	4195	1.100
	CS-2	CHS219.6 × 16	374	202	181	63.2	20	3640	0.947
	CS-3	CHS219.6 × 16	374	202	176	62.4	50	3640	0.940
	CS-4	CHS273 × 10	412	204	180	63.1	0	4195	0.987
	CS-5	CHS273 × 10	412	204	184	63.8	50	4450	1.055
	CS-6	CHS273 × 16	401	203	180	63.1	50	4450	0.971
	SS-1	SHS200 × 12.5	465	206	183	63.6	20	3640	0.968
	SS-2	SHS200 × 12	756	199	176	62.4	50	3640	1.057
	SS-3	SHS200 × 12	756	199	177	62.5	50	3640	1.058

*CHS = Circular Hollow Section; SHS = Square Hollow Section; f_{ys} and f_c denote steel tube yield strength and concrete compressive strength. E_s and E_c refer to the steel and concrete elastic modulus; e_0 refers to load eccentricity and L refers to specimen length for short columns and effective length for long columns

The structural test including circular and square cross-sections was carefully planned. Short column covers wide range of steel yield strength from 300 MPa to 779 MPa, while the concrete compressive strength remains very high within the range of 147 MPa to 193 MPa. In addition to the assessment of ultimate resistance and deformation capacity, confining efficiency for ultrahigh strength concrete were also analyzed by comparing the tested peak strength with plastic cross-section resistance calculated by EC4 (2004) with and without consideration of confinement.

For slender columns, both concentric and eccentric compression tests were conducted to obtain their buckling resistance. Special attention was placed on the consideration of initial imperfections and the reduction factor α_M (Xiong *et al*. 2017b). Since EC4 does not suggest suitable value of α_M when steel grade exceeds S460, a value of 0.8 is proposed for high strength steel beyond S460.

Test results were compared with EC4 prediction as plotted in Fig. 7. It should be noted that concrete confinement effect was conservatively neglected for both square and circular cross-sections, as the section slenderness ratio of steel tube was observed to exert great effect on the confining efficiency (Xiong *et al*. 2017a), and the brittleness of ultra-high strength makes the confinement much less significant than normal strength concrete (Wang *et al*. 2016). For the slender specimens, buckling curve “a” with magnitude of initial out-of-straightness equalling to L/300 was selected to represent the equivalent initial imperfection. As demonstrated in Fig. 6, the beam-column resistance was calculated by locating the point on M-N interaction diagram with equivalent bending moment as test result. Following the stipulation for S460 steel, the reduction factor α_M was assumed to be 0.8 for high strength steel.

As shown in Fig. 7, the average ratio of short column test result to EC4 prediction was 1.103 with standard deviation of 0.049. For slender column tests, more conservative prediction can be generated with average ratio of 1.163 and standard deviation of 0.098. Therefore, based on extensive of experimental proof, the current EC4 approach can be safely extended to high strength CFST columns with concrete compressive strength up to 180 MPa and steel yield strength up to 780 MPa. For design implementation, it is suggested that concrete confinement effect should be neglected and reduction factor α_M shall be taken as 0.8. It is noteworthy that a reduction factor η for high strength and ultra-high strength concrete was suggested by Liew and Xiong (2015, 2016) based on the analysis of more than 2030 test data, which allows for sufficient margin of safety as that of normal strength CFST columns. For concrete with characteristic compressive strength greater than 90 MPa, η = 0.8 is recommended. In addition, material compatibility must be checked to ensure that the steel section yield first prior to the crushing of concrete.

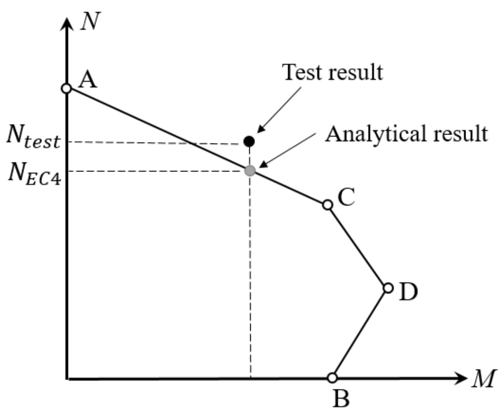

Fig. 6 Methodology to get EC4 predicted resistance for beam-column specimens

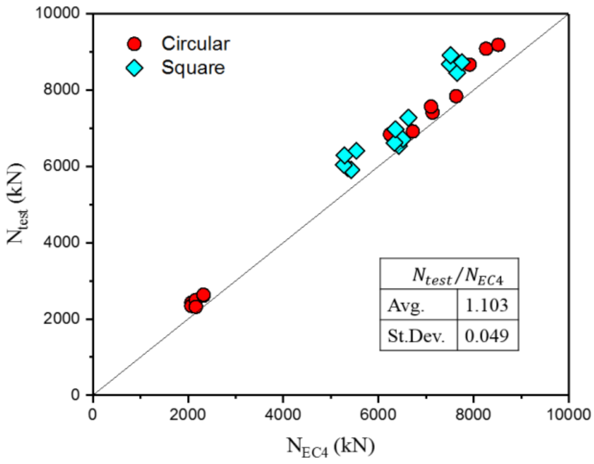

(a) Short column

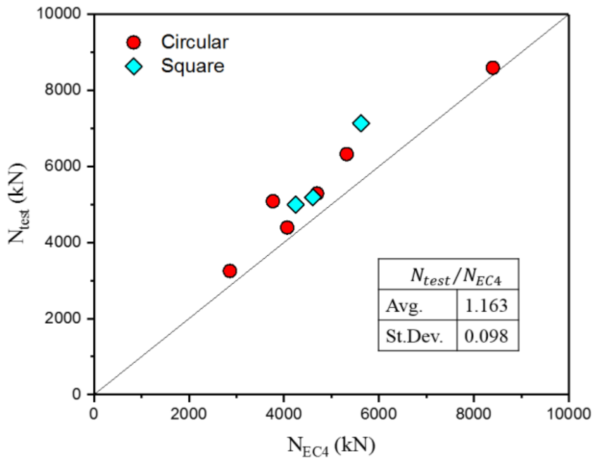

(b) Long column

Fig. 7 Comparison between test results (Xiong *et al*. 2017a, b) with EC4 prediction

4. Testing of high strength Concrete Encased Steel (CES) columns

4.1 Experimental program

Due to limited test data on high strength CES long column. Three CES specimens made of C100 concrete and S355 steel were tested. The cross-section size and thickness of the built-up steel section were proportionally scaled down from actual columns in a multi-storey building in Singapore. With the aim of investigating buckling behavior of high strength CES columns, all specimens were designed as long column with non-dimensional slenderness ratio ranging from 0.7 to 0.9, and concentric compression load was guaranteed by aligning the geometric centroid axis with the center line of pin-support as pictured in Fig. 8. The orientation of column specimens were properly arranged toensure buckling about minor axis. As summarized in Table 3, all specimens were 2800 mm long with buckling length of 3305 mm, which is taken as the distance between the rotational centre of top and bottom support. Concrete

Table 3 Details of CES long column specimens (Lai *et al*. 2019)

Specimen	CES1	CES2	CES3
Dimension B × D (mm × mm)	250×250	320×240	200×300
Steel section (mm)	130×115×14×22	126×113×13×20	100×100×6×10
Effective length L (mm)	3305	3305	3305
Link spacing (mm)	100	100	100
Non-dimensional slenderness	0.88	0.90	0.70
Concrete cylinder strength f_c (MPa)	96	96	96
Steel yield strength f_{ys} (MPa)	380	380	380
Main bar yield strength f_{yr} (MPa)	520	520	520
Main bar diameter φ_r (mm)	13	13	13
Link bar yield strength f_{yt} (MPa)	340	340	340
Link bar diameter φ_t (mm)	6	6	6
Section configuration	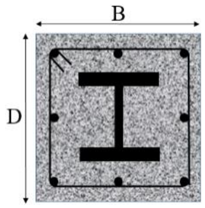	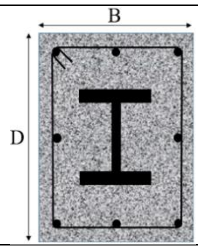	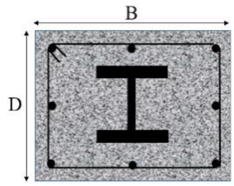

CES 1 CES 2 CES 3

Fig. 8 Test set-up and instrumentation of CES long column specimens

Table 4 Comparison of buckling resistance between test results and EC4 predictions

NO.	Test result (kN)	EC4 prediction (kN)					
	N_{test}	N_a	N_{test}/N_a	N_b	N_{test}/N_b	N_c	N_{tes}/N_c
CES1	5180	5535	0.94	4993	1.04	4534	1.14
CES2	6760	6155	1.10	5544	1.22	5028	1.34
CES3	5758	5166	1.11	4774	1.21	4413	1.30
Mean			1.05		1.15		1.26

[*] N_a, N_b and N_c refer to EC4 predicited result using Buckling Curve "a", "b" and "c" respectively

compressive cylinder strength was obtained at the same day of column test to accurately reflect basic material properties. More details of the experimental program can befound in Lai *et al*. (2019).

Initial imperfection for concentrically loaded members was implicitly considered by using the column buckling curve. Analytical prediction using buckling curve "a", "b" and "c" were compared with the test results in Table 4. It can be concluded that for CES columns with C100 concrete and S355 steel, EC4 gives conservative prediction of buckling resistance even though buckling curve "b" is used. However, in order to be consistent with normal strength CES column design, buckling curve "c" is recommended hence more conservative estimation can be generated.

Aside from physical test carried out by the authors (Lai *et al*. 2019), recent experimental work on high strength CES columns mainly focused on the behaviour of short columns and beam-columns. Table 5 summarizes the available specimen details reported in the literature. Zhu *et al*. (2014) conducted pure compression test on CES short columnswith normal strength steel S235 and high strength concrete C90. The parameters investigated in this study included reinforcement configuration, steel section shape and stirrup spacing. Different from Zhu *et al*. (2014), Kim *et al*. (2011, 2013) carried out eccentric compression test on beam-column specimens with C100 concrete and ultrahigh strength steel with yield strength exceeding 900 MPa. The load-carrying capacity was investigated by studying the effect of link spacing, load eccentricity, slenderness ratio and yield strength of lateral reinforcement. It was found the steel section did not yield when concrete crushed.

As shown in Table 6, most of specimens in Zhu *et al*. (2014) exhibit higher resistance than EC4 prediction except for specimen C-+-R40 with slight over-estimation of 3%, indicating the plastic resistance can be achieved if S235 steel and C90 concrete are used in CES short columns with I-section or cruciform steel section. As the ratio of test

Table 5 Details of high strength CES column specimens (Zhu *et al*. 2014, Kim *et al*. 2011, 2013)

Ref	Specimen	Dimension (B × D)	Steel section	f_c (MPa)	f_{ys} (MPa)	f_{yr} (MPa)	f_{yt} (MPa)	e_0 (mm)	L (mm)	S (mm)
Zhu *et al*. 2014	C-I-M40	200× 200	I10	93	254	427	335	0	600	40
	C-I-M60	200 × 200	I10	93	254	427	335	0	600	60
	C-I-R40	200 × 200	I10	93	254	427	335	0	600	40
	C-I-R60	200 × 200	I10	93	254	427	335	0	600	60
	C-+-M40	200 × 200	2 × I10	94	254	427	335	0	600	40
	C-+-M60	200 × 200	2 × I10	94	254	427	335	0	600	60
	C-+-M80	200 × 200	2 × I10	94	254	427	335	0	600	80
	C-+-R40	200 × 200	2 × I10	94	254	427	335	0	600	40
	C-+-R60	200 × 200	2 × I10	94	254	427	335	0	600	60
Kim *et al*. 2011	C1	260 × 260	150×100×17.6×17.6	94	913	525	560	120	2620	50
	C2	260 × 260	150×100×17.6×17.6	94	913	525	560	60	2620	50
	C3	260 × 260	150×100×17.6×17.6	94	913	525	560	120	2620	130
	C4	260 × 260	150×100×17.6×17.6	94	913	525	703	120	2620	50
Kim *et al*. 2013	C10	260 × 260	150×150×15×15	104	812	512	474	120	2620	65
	C11	260 ×x 260	150×150×15×15	104	812	512	474	120	3520	65

Table 6 Comparison between test results and EC4 predictions of CES short column (Zhu *et al*. 2014)

Specimen	ρ_l	ρ_v	ρ_s	N_{test} (kN)	N_{EC4} (kN)	N_{test}/N_{EC4}	Cross section
C-I-M40	2.36%	2.87%	3.58%	3862	3740	1.03	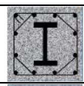
C-I-M60	2.36%	1.91%	3.58%	3789	3740	1.01	
C-I-R40	2.36%	1.95%	3.58%	3809	3740	1.02	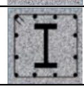
C-I-R60	2.36%	1.30%	3.58%	3838	3740	1.03	
C-+-M40	2.36%	2.87%	7.15%	4165	3990	1.04	
C-+-M60	2.36%	1.91%	7.15%	4104	3990	1.03	
C-+-M80	2.36%	1.44%	7.15%	4183	3990	1.05	
C-+-R40	2.36%	1.95%	7.15%	3855	3990	0.97	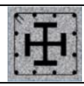
C-+-R60	2.36%	1.30%	7.15%	4010	3990	1.01	

*ρ_l, ρ_v and ρ_s refer to longitudinal reinforcement ratio, transverse reinforcement volumetric ratio and steel ratio, respectively

result to EC4 prediction is quite close to unity and no significant strength enhancement is achieved by reducing link spacing or improving reinforcement layout, concrete confinement effect shall be conservatively neglected for the purpose of design.

EC4 method could overestimate the buckling resistance of CES beam-columns according to the research by Kim *et al*. (2011, 2013). As shown in Fig. 9, the test results were all located within the axial force-bending moment interaction diagrams predicted by EC4 plastic design approach, indicating that the current EC 4 method could overestimate the resistance of beam columns with high strength materials. Liew *et al*. (Liew and Xiong 2015, Liew *et al*. 2016) pointed out the importance of material compatibility in composite column design. Since the yielding of ultra-high strength steel occurs only after concrete crushing, it is not possible to reply on inelastic redistribution of stress between steel and concrete and it is necessary to re-exam the applicability of plastic design in EC4, which will be discussed in detail in the later section.

5. Numerical analysis

5.1 Finite element model

The analytical study in Section 4 indicate that the existing EC4 method is not applicable in predicting the buckling resistance of CES beam-column members with high strength steel up to 900 MPa and high strength concrete up to 100 MPa, and this section investigates the behavior of high strength CES beam-columns using nonlinear finite element analysis. The test data collected by Kim *et al*. (2011, 2013) were used for verification. As

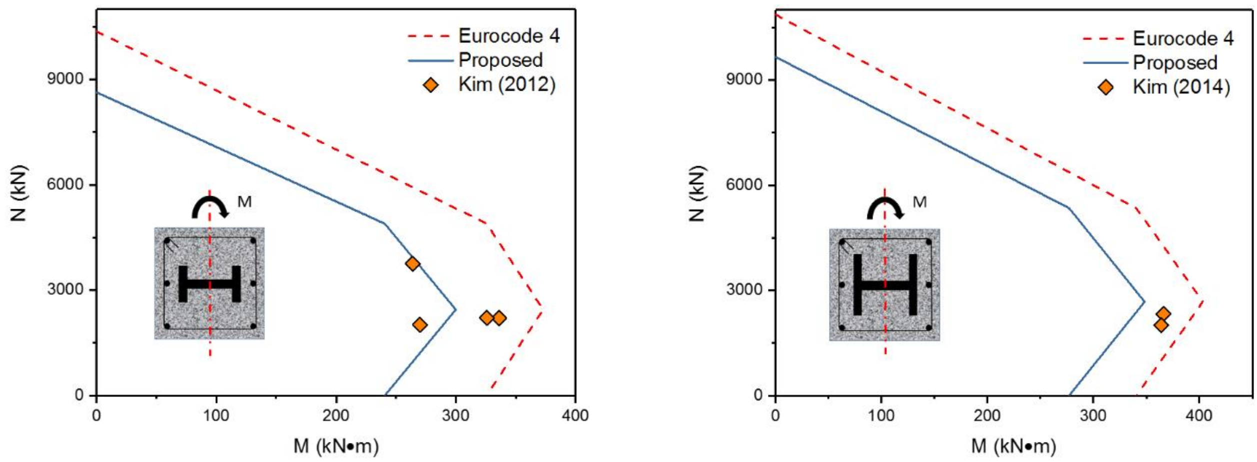

C1 - C4 C10 & C11

Fig. 9 Comparison between test results (Kim *et al*. 2011, 2013) and analytical prediction of CES beam-column

shown in Fig. 10, 8-node linear brick element with reduced integration C3D8R is selected for concrete and structural steel component, while the truss element T3D2 is used to capture the behavior of reinforcement bars, which were embedded in concrete encasement. The bond behavior ofsteel and concrete interface is simulated by defining a surface-to-surface contact and friction coefficient 0.25 is assumed as suggested by Ellobody *et al*. (Ellobody and Young 2011, Ellobody *et al*. 2011). In order to ensure the simultaneous load application on both steel and concrete, end plates were modeled at both ends and coupled to reference point positioning at the rotation center in the physical test. Pin-Pin support is simulated by releasing the rotational freedom about major axis for both top and bottom reference points, while the axial displacement of top reference point is set free to permit the displacement control in FEA.

For the material modelling, Concrete Damage Plasticity (CDP) is commonly adopted, which is capable of simulating the plastic behavior of concrete materials. Due to the high brittleness, the post-peak behavior of high strength plain concrete is not fully understood and the descending branch is hard to obtain in material test unless additional techniques is employed, such as applying active confining pressure or adding steel fibers. However, for numerical purpose, a complete stress-strain relation is required to capture the full range of load-deformation response. Thispaper used CEB model to represent material properties of HSC, which gives a steep descending branch and is applicable for HSC up to 100 MPa, more details of this model can be found in the cited papers (CEB1995, Güller *et al*. 2012).

5.2 Calibration of the finite element model

The load-deformation curves obtained from experimental investigation and numerical simulation are comparatively plotted in Fig. 11, from which it can be seen good agreement is reached in terms of initial stiffness, ultimate capacity, and post peak behavior. As indicated from these figures, all columns exhibit linear axial load-compressive strain relation until the attainment of peak load, followed by a sudden drop of axial load due to the concrete cover spalling and delamination, and then regain the load-carrying

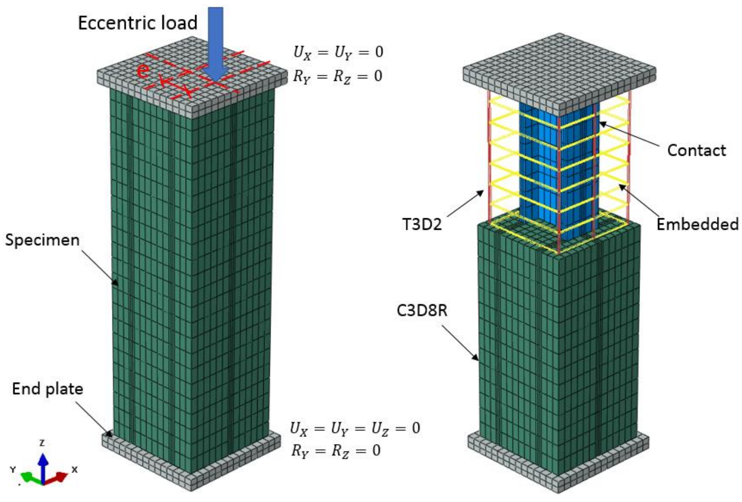

Fig. 10 Finite element model of CES columns

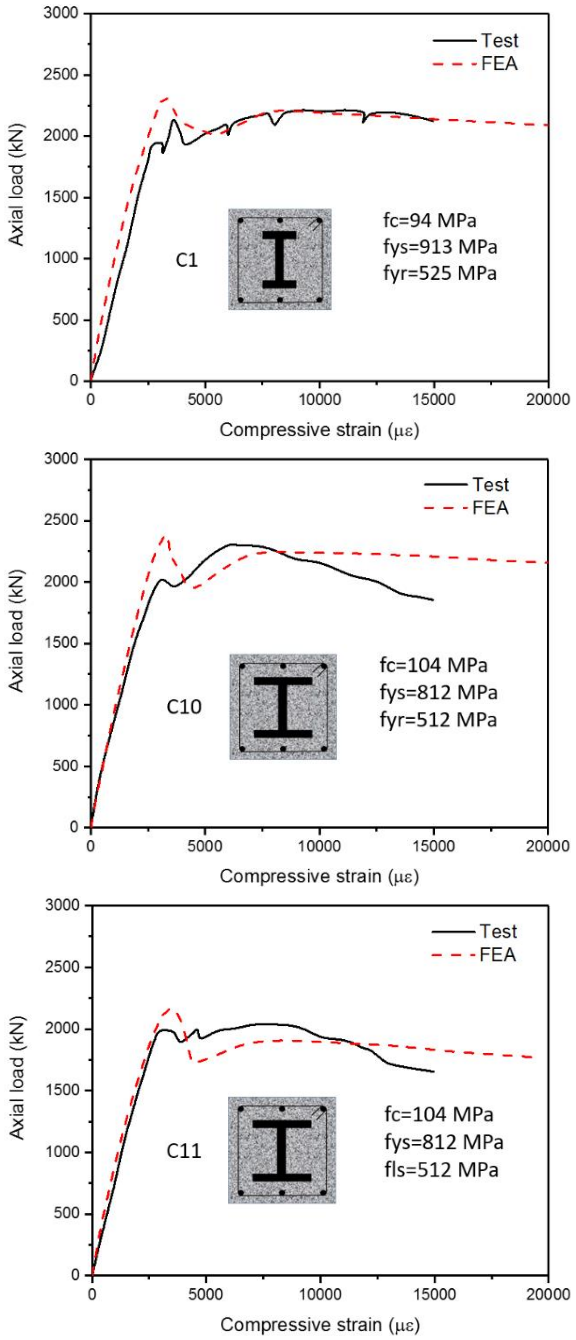

Fig. 11 Comparison between numerical and experimental results of axial load-compressive strain relation (Kim *et al*. 2011, 2013)

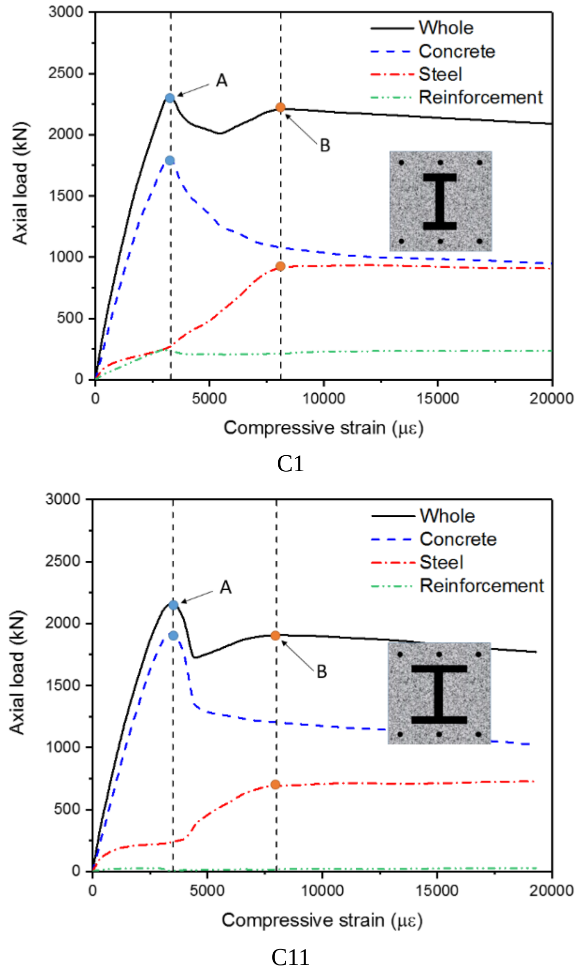

Fig. 12 Internal load distribution of each material component

capacity as the ultrahigh strength steel section still provide high resistance and then gradually yield with the increase of compressive strain after concrete spalling. The load displacement curves from the tests indicate that despite the usage of high strength concrete, noexplosive failure mode is observed and the post-peak behavior remains steady as shown in Fig. 11. This indicates that the brittleness of high strength concrete can be controlled by adopting closer spacing of transverse reinforcements in CES composite columns, and thepresence of highstrengthsteel section is able to provide sufficient post-peak strength after concrete cover spalling.

5.3 Behavioural studies

The axial force-compressive strain relation of each material component obtained from the numerical analysis isshown in Fig. 12. Two peak loads can be observed in the full range of load-deformation response. The first peak load "A" occurs when concrete component reaches the maximum capacity, while steel section is in the ascending branch and full plastic resistance has not yet achieved at this moment. After first peak load "A", concrete loss its resistance gradually due to concrete crush and steel stress continues to increase until the second peak load "B" is reached. It can be seen in Fig. 12 that the axial force carried by structural steel reaches the maximum at the second peak load "B", while the longitudinal reinforcing bars only carries small amount of axial force due to the large load eccentricity. For specimens C11, the reinforcing bars mainly resists the bending moment and the contribution to axial force is almost closed to 0. At point "B", the concrete component has entered into the descending branch since a large area of concrete was crushed into pieces and delaminated from the specimens. As visualized in Fig. 13, the failure mode observed in test is simulated by the numerical mode. The distribution of Equivalent Plastic Strain (PEEQ) in FEA model reasonably corresponds to the

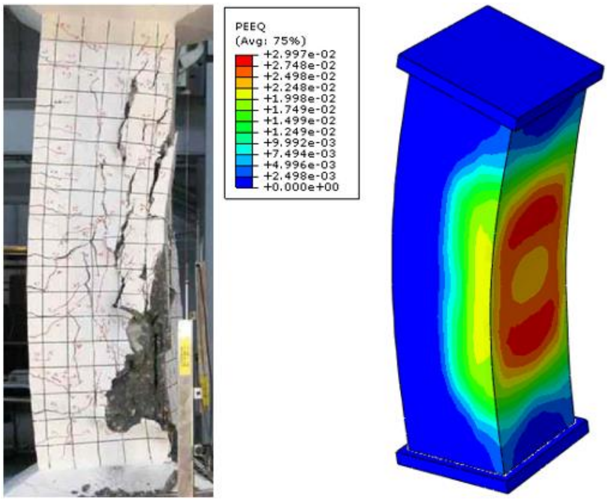

Fig. 13 Failure mode of specimen C1

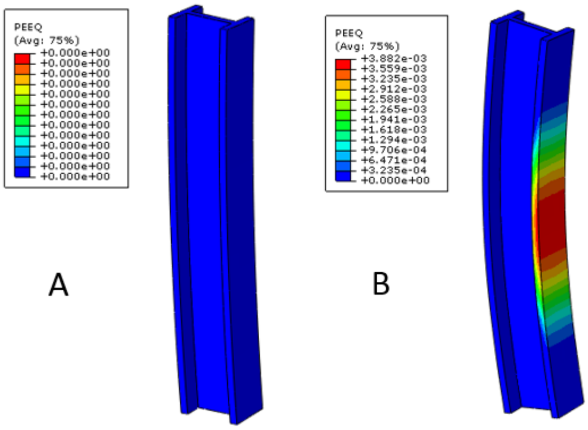

Equivalent plastic strain distribution

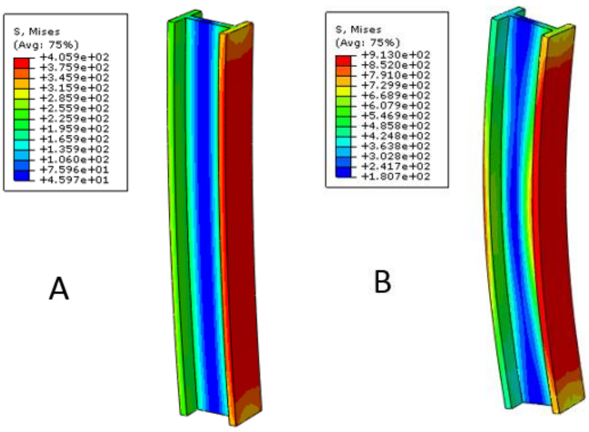

Von-Mises stress distribution

Fig. 14 Von Mises stress and equivalent plastic strain distribution of steel section C1 at first peak load (A) and second peak load (B)

concrete damage patterns in test.

The stress distribution of structural steel corresponding to the two peak loads are demonstrated in Fig. 14, it can be clearly seen the whole steel section does not achieve yield strength at the first peak load, but it yields at the second peak load instead, revealing that steel yielding occurs after the attainment of concrete peak strength, which does not conform to the stipulation of existing EC4 simplified method that concrete reaches the maximum strength after steel yielding.

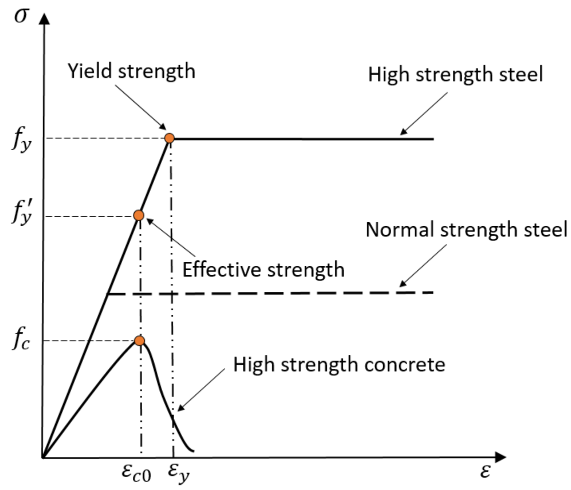

Fig. 15 Determination of effective strength for steel

6. Proposed analytical method

A new method based on effective strength of steel section is proposed for CES columns to trace the locus of axial force-bending moment interaction diagram. The proposed method is applicable to composite columns made of any combination of concrete and steel grades. To be consistent with the EC4 method of establishing the axial-moment (N-M) interaction curve, the proposed method also establishes the N –M curve using four anchor points linked by straight lines. The calculations procedure remains the same as that illustrated in Fig. 4, except for the determination on effective strength for steel section and longitudinal reinforcement.

The difference between high strength and normal strength steel section is compared in Fig. 15. For the ease of calculation, elastic-perfectly plastic stress-strain relation of steel is assumed. It can be seen that normal strength steel is able to reach yield strength before concrete reaches the maximum strength, whereas the high strength counterpart is still in elastic stage even though the peak strain of concrete is achieved, which is also verified in FEA as aforementioned. In order to address such a material incompatibility issue, the effective strength of steel component is adopted based on the concrete peak strain and computed using the expression below

$$f_y' = min(\,0.7E_a(f_{ck}+8)^{0.31}, f_y) \tag{7}$$

where f_{ck} refers to characteristic cylinder compressive strength of concrete, E_a refers to elastic modulus, which is taken as 210 GPa for structural steel section (EN1993-1-1 2005) and 200 GPa (EN1992-1-1 2004) for reinforcing steel bars.

Adopting the effective strength of steel component computed from Eq. (7), the M-N interaction diagram can be reconstructed as plotted in Fig. 9, and the coefficient $\alpha_M$is also taken as 0.8 for high strength steel S800 and S900. Material partial factors are set to be 1.0 for comparing with test results. It can be observed that the test result are all located outside or falls onto the newly constructed M-N envelope except for specimen C3, which lacks sufficient confinement due to the large spacing of transverse reinforcement (Kim *et al*. 2011), and this caused premature failure due to brittle crushing of the high strength concrete. The present findings point to the effectiveness of the proposed method in estimating CES beam columns made of high strength concrete, in particularly if the concrete reaches it maximum compressive strength first before steel yielding.This method is based on the assumption that sufficient shear links are provided to prevent premature failure of unconfined high strength concrete due to its brittle behavior, which is a subject of further research.

7. Conclusions

This paper presents a unified approach based on modified Eurocode 4 method to design Concrete Encased Steel (CES) composite columns with high strength steel and high strength concrete. Previous work on Concrete Filled Steel Tubular (CFST) columns has been reviewed and recent experimental work relevant to high strength CES column was added, followed by a nonlinear Finite Element Analysis (FEA) studying the behavior of high strength CES beam-columns. Eurocode 4 approach was carefully studied to verify its accuracy in predicting the load-carrying capacity of composite beam-columns made of high strength materials. Based on the strain compatibility criterion, M-N interaction diagram of high strength CES member is re-evaluated by replacing yield strength of steel with effective strength computed from the strain compatibility criterion. The conclusions from the research findings are summarized below:

- According to experimental study, the compression resistance of concrete filled tubular cross-section (i.e., short column) with concrete compressive strength from 150 to 190 MPa and steel yield strength from 300 to 780 MPa can be conservatively predicted by EC4 method. However, strength enhancement arising from concrete confinement effect should be neglected for design purpose as the confining efficiency is greatly affected by the slenderness of steel tube and brittleness of ultra-high strength concrete.
- For CFST beam-column members (i.e., slender member) with concrete strength 180 MPa and steel yield strength 780 MPa, it is proposed that a reduction factor η for high strength concrete and a reduction coefficient α_M for high strength steel shall be introduced, which provides conservative estimation of CFT beam-column members with sufficient margin of safety. Material compatibility rule should be obeyed to ensure that the steel section will yield before the crushing of the concrete, so that EC4 method can be used.
- Based on the test data, concrete encased steel (CES) short columns with C90 concrete and normal strength steelS235 is able to achieve full plastic resistance, and the current EC4 method gives good estimation of the compressive resistance. The reinforcement configuration and link spacing does not affect too much on the ultimate resistance of short columns but closer link spacing improves the post-peak behavior and ductility.
- The current EC4 method is capable of predicting the buckling resistance for CES long columns with concrete grade C90 and steel grade S355. For CES beam columns with concrete compressive strength of 100 MPa and steel yield strength up to 900 MPa, a modified EC4 approach, which is based on the strain compatibility method to determine the effective strength of steel section, can estimate the bending moment-axial force interaction curve with good accuracy. The proposed method provides a safe estimate on the beam-column resistance for CES members made of high strength steel and high strength concrete.

Future work will focus on the investigation of the effectiveness of shear links to provide proper confinement to high strength concrete to prevent early crushing of the concrete cover, which may affect the load carrying capacity of CES columns.

Acknowledgments

The authors would like to acknowledge the research grant R-302-000-168-490 from Building & Construction Authority of Singapore in supporting the work done in this paper. The test specimens prepared and donated by Penta-Ocean Construction Co. Ltd are gratefully acknowledged.

References

AIJ (1997), Recommendations for design and construction of concrete filled steel tubular structures; Architectural Institute of Japan; Japan. [In Japanese]

ANSI/AISC 360-16 (2016), Specification for Structural Steel Buildings, American Institute of Steel Construction (AISC); Chicago, IL, USA.

CEB high performance concrete (1995), Bull. D'information No. 228. Lausanne; 46P.

Chen, C.C. and Lin, N.J. (2006), "Analytical model for predicting axial capacity and behavior of concrete encased steel composite stub columns", *J. Constr. Steel Res.*, **62**(5), 424-433. https://doi.org/10.1016/j.jcsr.2005.04.021

Chen, C.C. and Yeh, S.C. (1996), "Ultimate strength of concrete encased steel composite columns",*Proceedings of the Third National Conference on Structural Engineering*: 2197-206. (in Chinese)

Du, Y.S., Chen, Z.H. and Xiong, M.X. (2016), "Experimental behavior and design method of rectangular concrete-filled tubular columns using Q460 high-strength steel", *Constr. Build. Mater*., **125**, 856-872. https://doi.org/10.1016/j.conbuildmat.2016.08.057

Du, Y.S., Chen, Z.H., Liew, J.Y.R. and Xiong, M.X. (2017), "Rectangular concrete-filled steel tubular beam-columns using high-strength steel: experiments and design", *J. Constr. Steel Res*., **131**, 1-8.https://doi.org/10.1016/j.jcsr.2016.12.016

Ellobody, E. and Young, B. (2011), "Numerical simulation of concrete encased steel composite columns", *J. Constr. Steel Res.*, **67**(2), 211-222.https://doi.org/10.1016/j.jcsr.2010.08.003

Ellobody, E., Young, B. and Lam, D. (2011), "Eccentrically loaded concrete encased steel composite columns", *Thin-Wall.Struct.*, **49**(1), 53-65.https://doi.org/10.1016/j.tws.2010.08.006

El-Tawil, S. and Deierlein, G.G. (1999), "Strength and ductility of concrete encased composite columns", *J. Struct. Eng.*, **125**(9), 1009-1019. https://doi.org/10.1061/(ASCE)0733-9445(1999)125:9(1009)

EN 1992-1-1 (2004), Eurocode 2: Design of Concrete Structures-Part 1-1. General Rules and Rules for Buildings, European Committee for Standardization; Brussels, Belgium.

EN 1993-1-1 (2005), Eurocode 3: Design of Steel Structures-Part 1-1. General Rules and Rules for Buildings, European Committee for Standardization; Brussels, Belgium.

EN 1994-1-1 (2004), Eurocode 4: Design of Composite Steel and Concrete Structures-Part 1-1. General Rules and Rules for Buildings,European Committee for Standardization; Brussels, Belgium.

Fenollosa, E., Gil, E., Cabrera, I. and Vercher, J. (2015), "Elastic-plastic formulation for concrete encased sections interaction diagram tracing", *Steel Compos. Struct., Int. J.*, **19**(4), 861-876. https://doi.org/10.12989/scs.2015.19.4.861

Güler, K., Demir, F. and Pakdamar, F. (2012), "Stress–strain modelling of high strength concrete by fuzzy logic approach", *Constr. Build. Mater.*, **37**, 680-684. https://doi.org/10.1016/j.conbuildmat.2012.07.069

Han, L.H., Zhao, X.L. and Tao, Z. (2001), "Tests and mechanics model for concrete-filled SHS stub columns, columns and beam-columns", *Steel Compos. Struct., Int. J.*, **1**(1), 51-74. https://doi.org/10.12989/scs.2001.1.1.051

Han, L.H., Yao, G.H. and Tao, Z. (2007), "Performance of concrete-filled thin-walled steel tubes under pure torsion", *Thin-Wall. Struct.*, **45**(1), 24-36. https://doi.org/10.1016/j.tws.2007.01.008

Hanswille, G., Bergmann, M. and Bergmann, R. (2017), "Design of composite columns with cross-sections not covered by Eucocode 4", *Steel Constr.*, **10**(1), 10-16. https://doi.org/10.1002/stco.201710004

JGJ 138-2016 (2016), Code for design of composite structures, Ministry of Housing and Urban-Rural Development of the People's Republic of China, China. [In Chinese]

Johansson, M. and Gylltoft, K. (2001), "Structural behavior of slender circular steel-concrete composite columns under various means of load application", *Steel Compos. Struct., Int. J.*, **1**(4), 393-410.https://doi.org/10.12989/scs.2001.1.4.393

Kim, D.K. (2005),"A database for composite columns", Master Dissertation; Georgia Institute of Technology, Atlanta, GA, USA.

Kim, C.S., Park, H.G., Chung, K.S. and Choi, I.R. (2011), "Eccentric axial load testing for concrete-encased steel columns using 800 MPa steel and 100 MPa concrete", *J. Struct. Eng.*, **138**(8), 1019-1031. https://doi.org/10.1061/(ASCE)ST.1943-541X.0000533

Kim, C.S., Park, H.G., Chung, K.S. and Choi, I.R. (2013), "Eccentric axial load capacity of high-strength steel-concrete composite columns of various sectional shapes", *J. Struct. Eng.*, **140**(4), 04013091. https://doi.org/10.1061/(ASCE)ST.1943-541X.0000879

Lai, B.L., Liew, J.Y.R. and Li, S. (2018), "Finite element analysis of concrete-encased steel composite columns with off-center steel section", *Proceedings of the 12th International Conference on Advances in Steel-Concrete Composite Structures*, ASCCS 2018, Valencia, June, pp. 297-303.

Lai, B.L., Liew, J.Y.R. and Wang, T.Y. (2019), "Buckling behaviour of high strength concrete encased steel composite columns", *J. Constr. Steel Res.*, **154**, 27-42. https://doi.org/10.1016/j.jcsr.2018.11.023

Lam, D. and Williams, C.A. (2004), "Experimental study on concrete filled square hollow sections", *Steel Compos. Struct., Int. J.*, **4**(2), 95-112.https://doi.org/10.12989/scs.2004.4.2.095

Liew, J.Y.R. and Xiong, M.X. (2015), "Design guide for concrete filled tubular members with high strength materials – an extension of Eurocode 4 method to C90/105 concrete and S550 steel", Research Publishing, Sinapore.

Liew, J.Y.R., Xiong, M.X. and Xiong, D.X. (2016), "Design of concrete filled tubular beam-columns with high strength steel and concrete", *Structures*, **8**, 213-226. https://doi.org/10.1016/j.istruc.2016.05.005

Liu, S.W., Liu, Y.P. and Chan, S.L. (2012), "Advanced analysis of hybrid steel and concrete frames: part 1: cross-section analysis technique and second-order analysis", *J. Constr. Steel Res.*, **70**, 326-336.https://doi.org/10.1016/j.jcsr.2011.09.003

Munoz, P.R. and Hsu, C.T. (1997), "Biaxially loaded concrete-encased composite columns: design equation", *J. Struct. Eng.*, **123**(12), 1576-1585. https://doi.org/10.1061/(ASCE)0733-9445(1997)123:12(1576)

Roik, K. and Bergmann, R. (1990), "Design method for composite columns with unsymmetrical cross-sections", *J. Constr. Steel Res.*, **15**, 153-168. https://doi.org/10.1016/0143-974X(90)90046-J

Tokgoz, S. and Dundar, C. (2008), "Experimental tests on biaxially loaded concrete-encased composite columns", *Steel Compos. Struct., Int. J.*, **8**(5), 423-438. https://doi.org/10.12989/scs.2008.8.5.423

Tsai, K.C., Lien, Y. and Chen, C.C. (1996), "Behaviour of axially loaded steel reinforced concrete columns", *J. Chinese Inst. Civil Hydraulic Eng.*, **8**(4), 535-545. [In Chinese]

Uy, B. (2001), "Axial compressive strength of short steel and composite columns fabricated with high strength steel plate",*Steel Compos.Struct*., *Int. J*., **1**(2), 171-185. https://doi.org/10.12989/scs.2001.1.2.171

Wang, Y.B., Liew, J.Y.R., Lee, S.C. and Xiong, D.X. (2016), "Experimental Study of Ultra-High-Strength Concrete under Triaxial Compression", *ACI Mater. J.*, **113**(1), 105-112.

Xiong, M.X., Xiong, D.X. and Liew, J.Y.R. (2017a), "Axial performance of short concrete filled steel tubes with high-and ultra-high-strength materials", *Eng. Struct*., **136**, 494-510. https://doi.org/10.1016/j.engstruct.2017.01.037

Xiong, M.X., Xiong, D.X. and Liew, J.Y.R. (2017b), "Behaviour of steel tubular members infilled with ultrahigh strength concrete", *J. Constr. Steel Res*., **138**, 168-183. https://doi.org/10.1016/j.jcsr.2017.07.001

Zhu, W.Q., Meng, G. and Jia, J.Q. (2014), "Experimental studies on axial load performance of high-strength concrete short columns", *Proceedings of the Institution of Civil Engineers-Structures and Buildings*, **167**(9), 509-519.

BU